Kinetics and Mechanism for Formation of Olefin Complexes in the Reaction between Palladium(II) and Maleic Acid

Tiesheng Shi and Lars I. Elding*

Inorganic Chemistry 1, Chemical Center, Lund University, P.O. Box 124, S-221 00 Lund, Sweden

Received January 22, 1998

Complex formation between $Pd(H_2O)_4^{2+}$ and maleic acid (H_2A) has been studied at 25 °C and 2.00 M ionic strength in acidic aqueous solution. Reaction takes place with 1:1 stoichiometry. The kinetics has been followed by use of stopped-flow spectrophotometry under pseudo-first-order conditions with maleic acid in excess. In the concentration ranges $0.01 \leq [H_2A]_{tot} \leq 0.50$ M and $0.40 \leq [H^+] \leq 2.00$ M, kinetic traces are biphasic. The biphasic kinetics and the dependence of reaction rate on pH and maleic acid concentration are rationalized in terms of a complex reaction mechanism of the type $\mathbf{A} \rightleftarrows \mathbf{B} \rightarrow \mathbf{C}$ where, in addition, both steps contain contributions from parallel reactions. The amplitude of the first phase increases with increasing $[H_2A]_{tot}$ and with decreasing $[H^+]$. Multiwavelength global analysis of the kinetic traces and the UV−vis spectral changes suggest that a monodentate oxygen-bonded hydrogen maleate complex, $[Pd(H_2O)_3OOCCH{=}CHCOOH]^+$, **B**, with stability constant $K_2 = 205 \pm 40$ M^{-1} is formed as an intermediate in this first step via two parallel reversible reactions in which $Pd(H_2O)_4^{2+}$ reacts with maleic acid and hydrogen maleate, respectively. In the following step, $\mathbf{B} \rightarrow \mathbf{C}$, slow intramolecular ring closure with a rate constant of 0.8 ± 0.1 s^{-1} at 25 °C gives the reaction product **C**, which is concluded to be a 4.5-membered olefin−carboxylato chelate complex on the basis of stoichiometry and UV−vis/NMR spectra. Parallel and irreversible attack by maleic acid and hydrogen maleate acting as olefins on the intermediate **B** also leads to formation of **C**. **C** is stable for at least 20 h for concentrations of ≤2 mM. Global multiwavelength analysis and simulations show that accumulation of the intermediate **B** is between ca. 2% and 60% depending on pH and concentration of maleic acid. Neither a steady-state approximation nor a rapid preequilibrium assumption can be used for the kinetics data treatment. Exact rate expressions for the fast and slow phases have been used to derive all rate constants involved. Olefins are inefficient nucleophiles toward palladium(II), even less efficient than carboxylic acids and carboxylates.

Introduction

In the context of a systematic study of structure−reactivity correlations for reactions between palladium(II) and carboxylic acids,[1,2] we have investigated the kinetics and mechanism for the reaction between $Pd(H_2O)_4^{2+}$ and maleic acid. This reaction results in a stable palladium(II) maleate complex with 1:1 stoichiometry, in contrast to the fast redox processes observed with simpler olefins.[3,4] The maleic acid molecule, having a cis configuration, may act as an ambidentate nucleophile through its two carboxylic groups as well as through its C=C double bond. This property helps to stabilize the reaction product but at the same time gives rise to an unusually complex reaction mechanism, involving consecutive and parallel reactions and slow and fast ring closure steps. The aim of the present study was to resolve this complex kinetics into its elementary processes. Some explanatory experiments using fumaric acid with a trans configuration, excluding the possibility of formation of a chelate bis(carboxylato) complex, and dimethyl maleate, which can only act as a nucleophile through its double bond, have also been performed in order to further elucidate the reaction mechanism.

Experimental Section

Chemicals and Solutions. Stock solutions of tetraaquapalladium(II) perchlorate (ca. 50 mM) in 2.00 M $HClO_4$ were prepared from palladium sponge (Johnson and Matthey, Spec. Pure) and analyzed spectrophotometrically as described previously.[5] For NMR measurements, stock solutions of 0.5 M $Pd(H_2O)_4^{2+}$ in concentrated perchloric acid (11.6 M) were used. Stock solutions of 2.000 and 4.00 M perchloric acid were prepared from concentrated perchloric acid (Merck, p.a.), and stock solutions of 2.000 M sodium perchlorate, from $NaClO_4 \cdot H_2O$ (Merck, p.a.). D_2O (99.5%), maleic acid (*cis*-HOOCCH=CHCOOH, p.a., 99%), fumaric acid (*trans*-HOOCCH=CHCOOH, p.a., 99%), and dimethyl maleate (*cis*-MeOOCCH=CHCOOMe, p.a., 96%), all from Janssen, were used as received without further purification. The ionic strength was 2.00 M in all kinetics experiments with 2.00 M $(H,Na)ClO_4$ as supporting electrolyte. Water was doubly distilled from quartz.

Apparatus. UV−vis spectra were recorded by use of a Milton Roy 3000 diode-array spectrophotometer and 1.00 cm quartz Suprasil cells. ^1H and ^{13}C NMR spectra were recorded on a Varian UNITY 300 spectrometer, and 2D NMR spectra (^{13}C vs ^1H) were recorded on a Bruker AMX 500 MHz spectrometer working at room temperature. The chemical shifts were measured in ppm by internal standards. Time-resolved UV−vis spectra were collected on an Applied Photophysics Bio Sequential SX-17 MV stopped-flow ASVD spectrofluorimeter. The kinetics was followed at 25.0 ± 0.1 °C by use of the Applied Photophysics instrument or a modified Durrum−Gibson stopped-flow spectrophotometer. Rate constants were evaluated by use of the Applied Photophysics software[6] or the OLIS nonlinear least-squares minimizing kinetics program Model 4000 Data System Stopped-flow Version 9.04.[7] Multivariate analysis of kinetics data (absorbance−wavelength−time)

* Corresponding author. Fax: +46-46-2224439. E-mail: Lars I.Elding@inorg.lu.se.

(1) Shi, T.; Elding, L. I. *Inorg. Chem.* **1996**, *35*, 735−740.
(2) Shi, T.; Elding, L. I. *Inorg. Chem.* **1997**, *36*, 528−536.
(3) Shitova, N. B.; Matveev, K. I.; Obynochnyi, A. A. *Kinet. Katal.* **1971**, *12*, 1417−1425.
(4) Shitova, N. B.; Matveev, K. I.; Kuznetsova, L. I. *Izv. Sib. Otd. Akad. Nauk SSSR, Ser. Khim. Nauk* **1973**, 25−30.
(5) Elding, L. I. *Inorg. Chim. Acta* **1972**, *6*, 647−651.

10.1021/ic980072f CCC: $15.00
Published on Web 09/25/1998

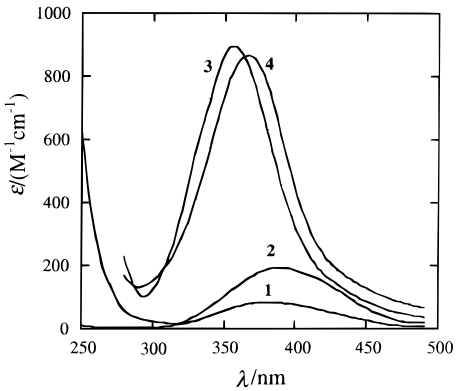

Figure 1. UV−vis spectra of Pd(II) complexes. (1) Spectrum of $Pd(H_2O)_4^{2+}$.[5] (2) Spectrum of $[Pd(H_2O)_3OOCCH_3]^+$.[1] (3) Spectrum developed by mixing 2.02 mM $Pd(H_2O)_4^{2+}$ and 2.4 mM maleic acid at $[H^+] = 1.00$ M. This corresponds to the maleate olefin complex **C**; cf. Scheme 1. (4) Spectrum developed by mixing 1.98 mM $Pd(H_2O)_4^{2+}$ and 14 mM fumaric acid at $[H^+] = 1.00$ M.

obtained by the SX-17MV spectrophotometer was performed by use of the global analysis (Glint) software.[8]

Protolysis Constants. Protolysis constants for maleic acid are $pK_{a1} = 1.7 \pm 0.1$ and $pK_{a2} = 5.60 \pm 0.03$ at 25 °C and 2.00 M ionic strength.[9] Under the present experimental conditions, i.e. $0.40 \le [H^+] \le 2.00$ M, the predominant species is maleic acid, whereas the concentration of hydrogen maleate is between 0.99 and 4.8 mol % and that of maleate can be neglected. The protolysis constant for $Pd(H_2O)_4^{2+}$ is $pK_h = 3.0 \pm 0.1$ at 25 °C and 1.00 M ionic strength.[10] Concentrations of palladium(II) hydroxo complexes can be neglected in the pH region studied.

Results

Stoichiometry. When solutions of 2−4 mM $Pd(H_2O)_4^{2+}$ are mixed with equal volumes of maleic acid solutions with total concentration $0.40 \le [H_2A]_{tot} \le 1000$ mM, complex formation is complete within a few seconds to a few minutes. After ca. 20 h, reduction to palladium(0) can be observed. Spectra of equilibrated solutions were recorded between 300 and 450 nm ca. 1 h after mixing. Plots of absorbance vs $[H_2A]_{tot}$ for $[H^+] = 1.00$ and 0.40 M indicate formation of a strong complex with 1:1 stoichiometry (Supporting Information).

Final Reaction Product. A UV−vis spectrum of the reaction product prepared by mixing 2.02 mM $Pd(H_2O)_4^{2+}$ and 2.4 mM maleic acid at $[H^+] = 1.00$ M is shown in Figure 1. Also included are spectra of $Pd(H_2O)_4^{2+}$ and $[Pd(H_2O)_3OOCCH_3]^+$. Formation of a monodentate oxygen-bonded palladium(II) maleate complex as the final product is expected to result in a spectrum resembling those of other palladium(II) carboxylato complexes (e.g., trace 2 in Figure 1).[1] This is obviously not the case. Formation of a seven-membered chelate complex bonded via the two carboxylate groups is also unlikely, since a solution of 1 mM $Pd(H_2O)_4^{2+}$ and 2 mM fumaric acid, which cannot form such a chelate complex, develops a similar spectrum (trace 3 in Figure 1). Moreover, equilibrium constants (defined as $K_1 = [Pd(H_2O)_3OOCR^+][H^+]/([Pd(H_2O)_4^{2+}][RCOOH])$) for reaction between $Pd(H_2O)_4^{2+}$ and a series of aliphatic carboxylic acids vary between 0.45 and 6.4.[2] Thus, these complexes are weak compared to the very strong complex observed in the present system. On the basis of these arguments, the complex formed as the final product is concluded to be an olefin complex.

Chart 1

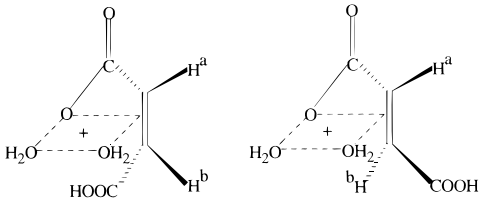

C

An ^1H NMR spectrum of a reaction mixture of ca. 20 mM Pd(II), 25 mM maleic acid, and 0.5 M $HClO_4$ in D_2O (Supporting Information) is stable for a few hours. A signal at 6.326 ppm can be assigned to free maleic acid. Coordinated maleic acid shows two inequivalent proton signals at ca. 4.2 ppm (H^a) and 3.3 ppm (H^b) with a coupling constant $^3J_{ab}^{cis} \approx 7$ Hz; cf. structures in Chart 1. A solution of 16 mM $Pd(H_2O)_4^{2+}$, 17 mM fumaric acid, and 0.30 M $HClO_4$ in D_2O displays a similar ^1H NMR spectrum with two doublets at ca. 4.3 ppm (H^a) and 2.5 ppm (H^b) with a coupling constant $^3J_{ab}^{trans} \approx 11$ Hz, in contrast to the only singlet at 6.86 ppm obtained for free fumaric acid. As observed before,[11,12] the chemical shifts of the protons attached to the double-bonded carbons move upfield on coordination. A 2D (^{13}C vs ^1H) NMR spectrum for the reaction (Supporting Information) shows that the alkene carbons in the complex resonate at higher fields ($\Delta\delta \approx 58$ and 107 ppm, respectively) than the free ones (131 ppm). The upfield movement to $\Delta\delta \approx 80$ ppm is a common feature for metal alkene complexes.[12−15] ^{13}C signals from the carboxylate groups were not observed since solutions were not stable long enough for accumulation.

The tentative structures of the final products formed in the reactions between $Pd(H_2O)_4^{2+}$ and maleic and fumaric acids based on the stoichiometry and the UV−vis and NMR spectra are given in Chart 1. These structures are further supported by the fact that reaction of $PdCl_4^{2-}$ with simple olefins does not give strong olefin complexes.[16−28] Coordination of the carboxylate to the metal center cis to the π bond seems to be geometrically feasible, although the structure might be sterically strained; strain could be released if the coordination of the C=C moiety is asymmetric, which is compatible with the NMR spectra. Similar structures have been proposed for intermediates in the oxidation of allyl alcohol and 2-cyclohexenol by $PdCl_4^{2-}$ in aqueous solution.[27,28]

It seems that there are no ^{13}C NMR data available in the literature for Pd(II)−olefin complexes in aqueous solution which are comparable to the marked upfield movement of $\Delta\delta \approx 107$ ppm observed here. The present NMR data could alternatively be interpreted in terms of a 5-coordinate structure with the carbon−carbon double bond located in an equatorial site and one carboxylate occupying an apical position.[29] This alternative

(6) *Applied Photophysics Bio Sequential SX-17 MV, Sequential Stopped-Flow ASVD Spectrofluorimeter, Software Manual*; Applied Photophysics Ltd.: Leatherhead, U.K., 1993.
(7) *OLIS kinetic fitting program*; OLIS Inc.: Jefferson, GA, 1987.
(8) King, P. J.; Maeder, M. *Glint-Global Kinetic Analysis*; Version 3.31; Applied Photophysics Ltd.: Leatherhead, U.K., 1993.
(9) Smith, R. M.; Martell, A. E. *Critical Stability Constants*; Plenum Press: New York, 1989; Vol. 6, 2nd Suppl., p 337.
(10) Shi, T.; Elding, L. I. *Acta Chem. Scand.* **1998**, *52*, 897−902.
(11) Hall, P. W.; Puddephatt, R. J.; Tipper, C. F. H. *J. Organomet. Chem.* **1974**, *71*, 145−151.
(12) Chaloner, P. A.; Davies, S. E.; Hitchcock, P. B. *J. Organomet. Chem.* **1997**, *527*, 145−154.
(13) Pellizer, G.; Lenarda, M.; Ganzerla, R.; Graziani, M. *Gazz. Chim. Ital.* **1986**, *116*, 155−161.
(14) Cooper, D. G.; Hughes, R. P.; Powell, J. *J. Am. Chem. Soc.* **1972**, *94*, 9244−9246.
(15) Chisholm, M. H.; Clark, H. C.; Manzer, L. E.; Stothers, J. B. *J. Am. Chem. Soc.* **1972**, *94*, 5087−5089.

appears less likely, however, since such 5-coordinate species are expected to be very unstable in aqueous solution.

Kinetics. Reactions were initiated by mixing equal volumes of the metal and ligand solutions directly in the stopped-flow instruments under pseudo-first-order conditions with maleic acid in excess. Kinetic traces are biphasic in the wavelength region 390−430 nm with one fast and one slow process, whereas they appear to be virtually monophasic for $\lambda < 390$ nm, where the amplitude of the initial fast reaction is small compared to that of the slow process. Most of the kinetics were monitored at 410 nm, where the best information about the fast phase can be obtained. At 410 nm and for high maleic acid and low hydrogen ion concentrations, the absorbance change of the initial process is sufficiently large, and the kinetics can be evaluated as two consecutive first-order processes with rate constants k^f_{obsd} and k^s_{obsd}, respectively, by use of a split-time base in recording the kinetic runs. At 360 nm, the kinetic traces can be described by single exponentials with rate constants k^s_{obsd} after exclusion of the first few data points. Rate constants k^s_{obsd}, measured at 360 nm, are in good agreement with those determined at 410 nm. Rate constants k^f_{obsd} and k^s_{obsd} as functions of pH and of maleic acid concentration are summarized in Supporting Information Table S1. Corresponding studies of the fumaric acid and dimethyl maleate reactions are not feasible because of solubility problems and slow kinetics.[30]

Global Analysis. The amplitude of the first phase of the reaction increases with increasing $[H_2A]_{tot}$ and with decreasing hydrogen ion concentrations, reflecting reversible formation of an intermediate in a reaction involving maleic acid and oxonium ions. Time-resoved spectra under conditions favorable for accumulation of the intermediate are given as Supporting Information. Single-value decomposition (SVD) calculations[8,31−33] by use of the multiwavelength kinetics data indicate that there are three absorbing species involved in the reaction. The observations suggest that the overall reaction can be represented by eq 1, where k_{12}, k_{21}, and k_{23} are pseudo-first-

$$\mathbf{A} \underset{k_{21}}{\overset{k_{12}}{\rightleftharpoons}} \mathbf{B} \xrightarrow{k_{23}} \mathbf{C} \qquad (1)$$

order rate constants and **A**, **B**, and **C** in this particular case denote $Pd(H_2O)_4^{2+}$, the intermediate, and the reaction product,

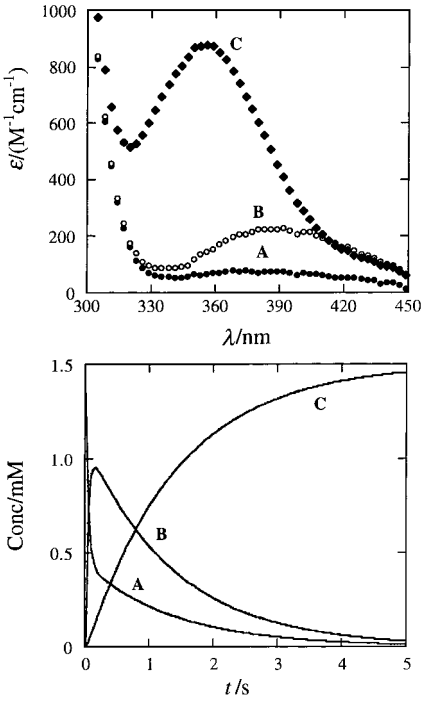

Figure 2. Spectra of **A**, **B**, and **C** in eq 1 and their concentration change with time obtained by global analysis of time-resolved spectra. Conditions for the concentration−time profiles: $[Pd(H_2O)_4^{2+}] = 1.50$ mM, $[H_2A]_{tot} = 0.50$ M, $[H^+] = 1.00$ M, 2.00 M ionic strength, and 25 °C.

respectively. Global analysis performed by fitting this reaction model to the experimental data reproduced perfectly all kinetic traces and time-resolved spectra. The calculated spectra of **A**, **B**, and **C** and their concentration changes as a function of time are shown in Figure 2. The spectrum of intermediate **B** is very similar to those of a series of monodentate carboxylato complexes of palladium(II) reported previously (e.g., spectrum 2 in Figure 1).[1,2] Thus, intermediate **B** is most likely the monodentate hydrogen maleate complex $[Pd(H_2O)_3OOCCH{=}CHCOOH]^+$.

Reaction Mechanism. The proposed reaction mechanism for the overall process is depicted in Scheme 1. Intermediate **B** is formed via reversible parallel reactions between $Pd(H_2O)_4^{2+}$ and maleic acid and hydrogen maleate. The relative concentration of **B** could amount to ca. 60 mol % during the course of reaction under some experimental conditions used (see Figure 2). Irreversible transformation of the oxygen-bonded intermediate **B** to the stable olefin complex **C** described by the overall rate constant k_{23} proceeds via three pathways. The direct and dominant route is a slow intramolecular ring closure, with rate constant k_{src}. In addition, the aqua ligand trans to the coordinated hydrogen maleate in **B** is labilized due to the trans effect of the carboxylato ligand. Such labilization might enable a second maleic acid molecule or hydrogen maleate ion to attack the trans position of **B** acting as olefins (attack by carboxylate forming a bis(carboxylato) complex is not thermodynamically feasible, since the stability constants for bis(carboxylato) complexes at this low pH are too small).[1,2] Subsequently, the oxygen-bonded hydrogen maleate will be rapidly substituted by water molecules due to the much larger trans effect of the coordinated olefin.[34] A fast ring closure reaction follows. The contribution from these two pathways, denoted by k_3 and k_4 in Scheme 1, depends on $[H_2A]_{tot}$ and $[H^+]$. The detailed mechanism is discussed below.

(16) Henry, P. M. *J. Am. Chem. Soc.* **1964**, *86*, 3246−3250.
(17) Henry, P. M. *J. Am. Chem. Soc.* **1966**, *88*, 1595−1597.
(18) Henry, P. M. *J. Org. Chem.* **1967**, *32*, 2575−2580.
(19) Henry, P. M. *J. Am. Chem. Soc.* **1972**, *94*, 4437−4440.
(20) Henry, P. M. *J. Org. Chem.* **1973**, *38*, 1681−1684.
(21) Moiseev, I. I.; Levanda, O. G.; Vargaftik, M. N. *J. Am. Chem. Soc.* **1974**, *96*, 1003−1007.
(22) Lee, H.-B.; Henry, P. M. *Can. J. Chem.* **1976**, *54*, 1726−1737.
(23) Henry, P. M. *J. Am. Chem. Soc.* **1972**, *94*, 7305−7310.
(24) Zaw, K.; Lautens, M.; Henry, P. M. *Organometallics* **1985**, *4*, 1286−1291.
(25) Zaw, K.; Henry, P. M. *J. Org. Chem.* **1990**, *55*, 1842−1847.
(26) Hamed, O.; Henry, P. M. *Organometallics* **1997**, *16*, 4903−4909.
(27) Wan, W. K.; Zaw, K.; Henry, P. M. *Organometallics* **1988**, *7*, 1677−1683.
(28) Zaw, K.; Henry, P. M. *Organometallics* **1992**, *11*, 2008−2015.
(29) Manzer, L. E. *Inorg. Chem.* **1976**, *15*, 2354−2357.
(30) The solubility of fumaric acid is ca. 30 mM, and its reaction with $Pd(H_2O)_4^{2+}$ is slow. At the final stage of the reaction, reduction of Pd(II) could be observed. Reaction between the Pd(II) complex and dimethyl maleate is also slow. It is not possible to calculate the observed rate constant, since protons catalyze the hydrolysis of dimethyl maleate.
(31) Maeder, M.; Zuberbühler, A. D. *Anal. Chem.* **1990**, *62*, 2220−2224.
(32) Beechem, J. M. *Methods Enzymol.* **1992**, *210*, 37−55.
(33) Stultz, L. K.; Binstead, R. A.; Reynolds, M. S.; Meyer, T. J. *J. Am. Chem. Soc.* **1995**, *117*, 2520−2532.
(34) Elding, L. I.; Gröning, Ö. *Inorg. Chem.* **1978**, *17*, 1872−1880.

Scheme 1. Proposed Reaction Mechanism for the Formation of Palladium(II) Hydrogen Maleate Complexes According to Eq 1[a]

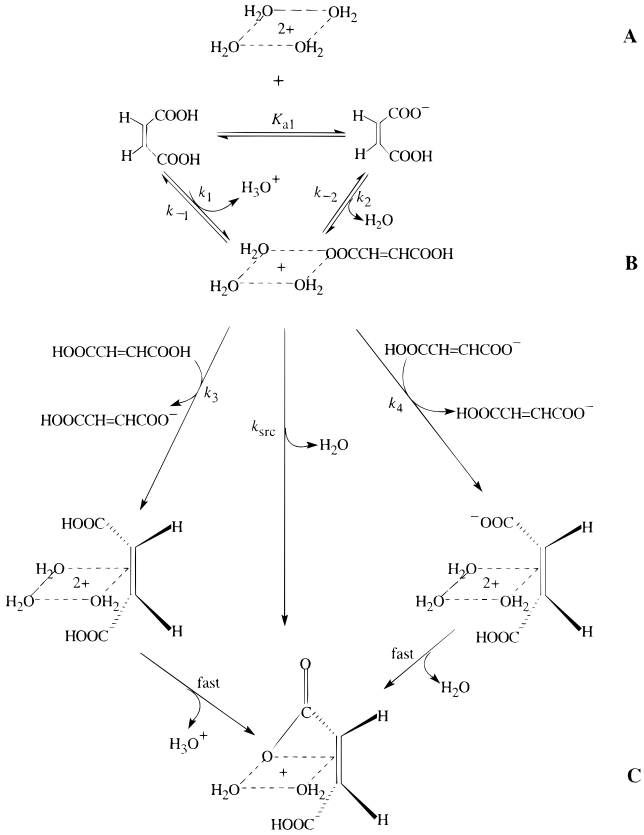

[a] Only one of the two possible mechanisms for the reactions described by k_3 and k_4 is indicated (cf. text).

Direct reaction between $Pd(H_2O)_4^{2+}$ and dimethyl maleate is very slow.[30] Since the olefinic properties of maleic acid and dimethyl maleate are similar, this observation suggests that direct attack by maleic acid or hydrogen maleate at $Pd(H_2O)_4^{2+}$ through the C═C double bond can be neglected.

By use of the reaction model in Scheme 1, the rate constants k_{12}, k_{21}, and k_{23} in eq 1 can be formulated as eqs 2−4. The

$$k_{12} = k_I[H_2A]_{tot} \tag{2a}$$

$$k_I = (k_1[H^+] + k_2K_{a1})/(K_{a1} + [H^+]) \tag{2b}$$

$$k_{21} = k_{-1}[H^+] + k_{-2} \tag{3}$$

$$k_{23} = k_{II}[H_2A]_{tot} + k_{src} \tag{4a}$$

$$k_{II} = (k_3[H^+] + k_4K_{a1})/(K_{a1} + [H^+]) \tag{4b}$$

exact solution for the mechanism described by eq 1 is shown in eqs 5 and 6.[35] With the initial conditions of $[\mathbf{A}]_0 = [Pd(II)]_{tot}$,

$$\lambda_2 = \{k_{12} + k_{21} + k_{23} + [(k_{12} + k_{21} + k_{23})^2 - 4k_{12}k_{23}]^{1/2}\}/2 \tag{5}$$

$[\mathbf{B}]_0 = 0$, and $[\mathbf{C}]_0 = 0$, the molar fractions of **A**, **B**, and **C** as a function of time can be derived as eqs 7−9.[35]

(35) Moore, J. W.; Pearson, R. G. *Kinetics and Mechanism. A Study of Homogeneous Chemical Reactions*, 3rd ed.; John Wiley & Sons: New York, 1981; p 313.

$$\lambda_3 = \{k_{12} + k_{21} + k_{23} - [(k_{12} + k_{21} + k_{23})^2 - 4k_{12}k_{23}]^{1/2}\}/2 \tag{6}$$

$$\frac{[\mathbf{A}]}{[Pd(II)]_{tot}} = \frac{k_{12}(\lambda_2 - k_{23})}{\lambda_2(\lambda_2 - \lambda_3)}\exp(-\lambda_2 t) + \frac{k_{12}(k_{23} - \lambda_2)}{\lambda_3(\lambda_2 - \lambda_3)}\exp(-\lambda_3 t) \tag{7}$$

$$\frac{[\mathbf{B}]}{[Pd(II)]_{tot}} = -\frac{k_{12}}{\lambda_2 - \lambda_3}\exp(-\lambda_2 t) + \frac{k_{12}}{\lambda_2 - \lambda_3}\exp(-\lambda_3 t) \tag{8}$$

$$\frac{[\mathbf{C}]}{[Pd(II)]_{tot}} = \frac{k_{12}k_{23}}{\lambda_2\lambda_3} + \frac{k_{12}k_{23}}{\lambda_2(\lambda_2 - \lambda_3)}\exp(-\lambda_2 t) - \frac{k_{12}k_{23}}{\lambda_3(\lambda_2 - \lambda_3)}\exp(-\lambda_3 t) \tag{9}$$

Calculation of Rate Constants. Combining of eqs 5 and 6 and introducing $k^f_{obsd} = \lambda_2$ and $k^s_{obsd} = \lambda_3$ give

$$k^f_{obsd} + k^s_{obsd} = \lambda_2 + \lambda_3 = k_{12} + k_{21} + k_{23} \tag{10}$$

$$k^f_{obsd}k^s_{obsd} = \lambda_2\lambda_3 = k_{12}k_{23} \tag{11}$$

Substitution of eqs 2−4 into eqs 10 and 11 leads to

$$k^f_{obsd} + k^s_{obsd} = (k_I + k_{II})[H_2A]_{tot} + k_{21} + k_{src} \tag{12}$$

$$k^f_{obsd}k^s_{obsd} = k_Ik_{II}[H_2A]_{tot}^2 + k_Ik_{src}[H_2A]_{tot} \tag{13}$$

Equation 12 suggests that plots of $k^f_{obsd} + k^s_{obsd}$ vs the total concentration of maleic acid should be linear; cf. Figure 3. The intercepts, $k_{21} + k_{src}$, and slopes, $k_I + k_{II}$, of these plots are listed in Table 1 (for $[H^+] = 2.00$ M, only two data points for k^f_{obsd} were obtained; these are not included in Figure 3). Plots of $k^f_{obsd}k^s_{obsd}$ as a function of $[H_2A]_{tot}$ are shown in Figure 4. A nonlinear least-squares analysis according to eq 13 gives excellent fits. The derived values of k_Ik_{II} and k_Ik_{src} are also included in Table 1.

The values of k_I and k_{II} given in Table 2 can be derived from the values of $k_I + k_{II}$ and k_Ik_{II}, (negative solutions for k_I and k_{II} are meaningless and can be neglected). These values in turn enable us to calculate k_{src} and k_{21} from those of k_Ik_{src} and of $k_{21} + k_{src}$ (cf. Table 2). It is noteworthy that the value of k_{src} is independent of $[H^+]$, as expected for an intramolecular ring closure reaction. k_{21} as a function of $[H^+]$ is analyzed by a linear least-squares fit according to eq 3, affording $k_{-1} = 4.6 \pm 0.2$ M^{-1} s^{-1} and $k_{-2} = 2.8 \pm 0.2$ s^{-1} at 25 °C. A nonlinear least-squares analysis of k_I and k_{II} as a function of $[H^+]$ according to eqs 2b and 4b, respectively, gives the values of k_1, k_2, k_3, and k_4. Values of all rate constants defined in Scheme 1 are summarized in Table 3.

By use of the rate constants in Table 3 and eqs 2−6, the observed pseudo-first-order rate constants for both the fast and slow phases were recalculated. Good agreement between observed and calculated rate constants is found for all conditions (cf. Supporting Information Table S1). Further, the rate constants in Table 3 together with eqs 7−9 can be utilized to simulate the time-dependent concentrations of the complexes. Simulation under the same conditions as used for the global analysis results in identical concentration vs time diagrams. An example is given in Figure 2. For $[H_2A]_{tot} = 0.010$ M and $[H^+] = 2.00$ M, the simulation shows that accumulation of **B** amounts

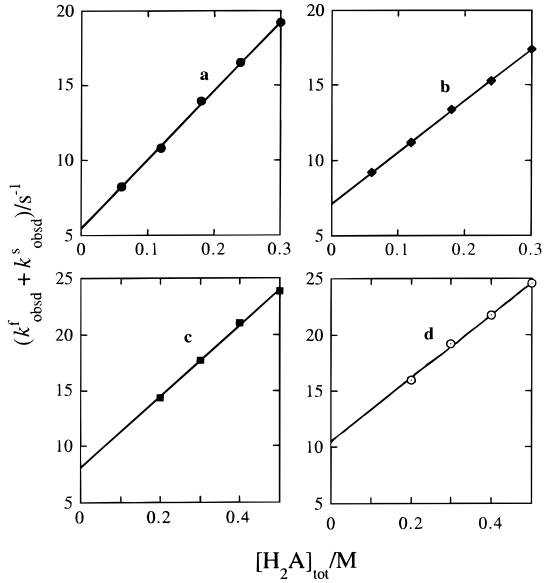

Figure 3. Plots of $(k^f_{obsd} + k^s_{obsd})$ vs $[H_2A]_{tot}$ according to eq 12 at 25 °C. $[H^+]$: (a) 0.40 M; (b) 0.70 M; (c) 1.00 M; (d) 1.50 M. Complete data are given as Supporting Information.

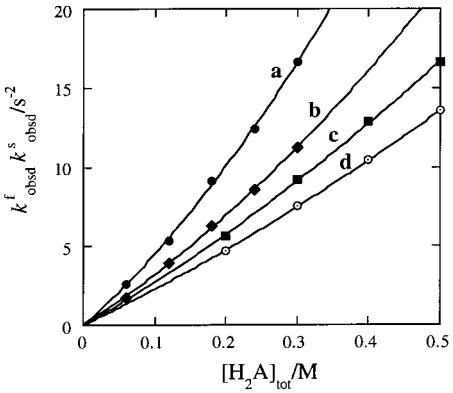

Figure 4. The product $k^f_{obsd}k^s_{obsd}$ as a function of $[H_2A]_{tot}$ at 25 °C. The solid lines represent the best fit of eq 13 to the experimental data by a nonlinear least-squares method. $[H^+]$: (a) 0.40 M; (b) 0.70 M; (c) 1.00 M; (d) 1.50 M.

Table 1. Values of $k_I + k_{II}$ and of $k_{21} + k_{src}$ Derived from Figure 3 and of k_Ik_{II} and k_Ik_{src} Derived from Figure 4 by Least-Squares Fitting of Eqs 12 and 13, Respectively

$[H^+]$/M	$(k_I + k_{II})$/ $(M^{-1}\ s^{-1})$	$(k_{21} + k_{src})$/ s^{-1}	k_Ik_{II}/ $(M^{-2}\ s^{-1})$	k_Ik_{src}/ $(M^{-1}\ s^{-2})$
0.40	46.0 ± 0.7	5.4 ± 0.7	51.8 ± 7.4	39.9 ± 1.9
0.70	34.1 ± 0.4	7.1 ± 0.1	27.8 ± 4.0	29.2 ± 1.0
1.00	31.9 ± 1.0	8.1 ± 0.4	15.4 ± 2.1	25.7 ± 0.9
1.50	28.3 ± 0.9	10.5 ± 0.3	11.1 ± 0.7	21.6 ± 0.3

Table 2. Values of k_I, k_{II}, k_{src}, and k_{21} Derived from the Data in Table 1

$[H^+]$/M	$k_I/(M^{-1}\ s^{-1})$	$k_{II}/(M^{-1}\ s^{-1})$	k_{src}/s^{-1}	k_{21}/s^{-1}
0.40	44.8 ± 2.7	1.16 ± 0.06	0.9 ± 0.1	4.5 ± 0.6
0.70	33.3 ± 2.3	0.84 ± 0.06	0.9 ± 0.1	6.2 ± 0.1
1.00	31.4 ± 2.1	0.50 ± 0.03	0.8 ± 0.1	7.3 ± 0.3
1.50	27.9 ± 0.8	0.40 ± 0.02	0.8 ± 0.1	9.7 ± 0.2

only to ca. 2%. This is why in such a case the first reaction phase can hardly be observed.

Discussion

The simulations demonstrate that the intermediate carboxylato complex **B** can accumulate from ca. 2 up to 60 mol % during the course of reaction depending on the concentration of maleic acid and pH. Based on the data in Tables 1 and 2, simple calculations show that k_{23} is comparable to k_{12} and k_{21} (cf. eq 1) under certain conditions. These facts indicate that neither a steady-state approximation for **B** nor an assumption of a rapid preequilibrium between **A** and **B** in eq 1 can be used for the kinetics data treatment.[36] Instead, the exact rate expressions, eqs 12 and 13, have to be used for the data analysis.

Table 3. Summary of Rate and Equilibrium Constants Defined by Scheme 1 at 25 °C and Ionic Strength 2.00 M

parameter	value	method	parameter	value	method
$k_1/(M^{-1}\ s^{-1})$	21.2 ± 1.3	eq 2b	$k_4/(M^{-1}\ s^{-1})$	22.8 ± 3.1	eq 4b
$k_{-1}/(M^{-1}\ s^{-1})$	4.6 ± 0.2	eq 3	k_{src}/s^{-1}	0.8 ± 0.1	Table 2
$k_2/(M^{-1}\ s^{-1})$	510 ± 40	eq 2b	K_1	4.6 ± 0.5	k_1/k_{-1}
k_{-2}/s^{-1}	2.8 ± 0.2	eq 3	K_2/M^{-1}	180 ± 30	k_2/k_{-2}
$k_3/(M^{-1}\ s^{-1})$	0.11 ± 0.09	eq 4b	K_2/M^{-1}	230 ± 30	K_1/K_{a1}

In the hydrogen ion concentration range used, the reactions between $Pd(H_2O)_4^{2+}$ and maleic acid and hydrogen maleate are sufficient to describe the formation of **B**, whereas the contribution from reactions with $Pd(H_2O)_3OH^+$ can be neglected due to the small protolysis constant of tetraaquapalladium(II).[10] Moreover, the derived equilibrium constant, $K_1 = k_1/k_{-1} = 4.6 \pm 0.5$, is very reasonable, since it falls within the range of K_1 values determined for a large series of other palladium(II) carboxylato complexes.[1,2] The stability constant $\beta_1 = K_2$ of **B** can be calculated independently as k_2/k_{-2} and as K_1/K_{a1}. The internal agreement between these values is satisfactory, giving an average value of $\beta_1 = 205 \pm 40\ M^{-1}$; cf. Table 3. Moreover, the values of β_1 for this carboxylato complex and pK_{a1} for maleic acid fit well into the linear free energy relation derived recently,[2] if differences in ionic strength are considered (see ref 2, Figure 7).

It has been observed earlier that rate constants for substitution reactions with carboxylic acids are virtually independent of the nature of the acids, ranging only between 9.0 and 21.1 $M^{-1}\ s^{-1}$.[2] In the present system, the entry of maleic acid with a rate constant of 21.2 ± 1.3 $M^{-1}\ s^{-1}$ is in good agreement with these observations.[2] Thus, the equilibrium, stability, and rate constants evaluated for the formation of intermediate **B** agree with previous results for the formation of palladium(II) monodentate carboxylato complexes.[2]

Crystal structures of monodentate hydrogen maleate complexes of for instance Mn(II),[37] Ni(II),[38,39] and Zn(II)[39] have been determined. Common to these structures is hydrogen bond formation between the hydroxyl group of the noncoordinated carboxylic group and the carbonyl oxygen of the coordinated carboxylate. Such hydrogen bonding might also stabilize the intermediate complex **B** suggested here.

The rate constant of $k_2 = 510 \pm 40\ M^{-1}\ s^{-1}$ is the first one obtained for a carboxylate anion reacting with the palladium(II) complex. The value is comparable to that for reaction between $Pd(H_2O)_4^{2+}$ and HSO_4^- ($119 \pm 6\ M^{-1}\ s^{-1}$)[10] but less than those of the corresponding reactions with halides[40,41] and thioethers.[42] The very slow reaction between $Pd(H_2O)_4^{2+}$ and dimethyl maleate, the negligible contribution to the overall process from a direct attack on the metal center by the C=C double bond of maleic acid/hydrogen maleate, and the small

(36) Espenson, J. H. *Chemical Kinetics and Reaction Mechanisms*, 2nd ed.; McGraw-Hill: New York, 1995; Chapter 4.
(37) Lis, T. *Acta Crystallogr.* **1983**, *C39*, 39−41.
(38) Gupta, M. P.; Geise, H. J.; Lenstra, A. T. H. *Acta Crystallogr.* **1984**, *C40*, 1152−1154.
(39) Sequeira, A.; Rajagopal, H. *Acta Crystallogr.* **1992**, *C48*, 1192−1197.
(40) Elding, L. I. *Inorg. Chim. Acta* **1972**, *6*, 683−688; **1978**, *28*, 255−262.
(41) Elding, L. I.; Olsson, L.-F. *Inorg. Chim. Acta* **1986**, *117*, 9−16.
(42) Shi, T.; Elding, L. I. *Inorg. Chem.* **1996**, *35*, 5941−5947.

values of k_3 and k_4 suggest that olefins are inefficient entering ligands, similar to what was observed for reactions with platinum(II) complexes.[43,44] In the case of maleic acid, nucleophilic attack via the carboxylic group is much more efficient than attack via the olefin bond.

The reactions described by k_3 and k_4 in Scheme 1 proceed as bimolecular processes with maleic acid and hydrogen maleate acting as olefins, attacking intermediate **B** in parallel reactions. There are at least two possible reaction mechanisms that can be used to rationalize the k_3 pathway.[44−46] (i) Displacement of the trans water molecule in the intermediate by maleic acid acting as an olefin could form a new intermediate, *trans*-[Pd(H$_2$O)$_2$(HOOCC═CHCOOH)(HOOCCH═CHCOO)]$^+$. Subsequently, the oxygen-bonded hydrogen maleate in this complex will be rapidly replaced by water molecules due to the large trans effect of olefin, followed by a fast ring closure to form **C**. (ii) Alternatively, attack on intermediate **B** by maleic acid might involve formation of a trigonal-bipyramidal activated complex with the entering maleic acid, the leaving oxygen-bonded hydrogen maleate and the trans water molecule in the equatorial plane. After loss of the oxygen-bonded hydrogen maleate, fast ring closure gives the olefin complex **C**. These possibilities are also applicable to the k_4 pathway in Scheme 1. Together, these two pathways contribute less than 26% to k_{23} under the conditions used. However, eqs 12 and 13 cannot be fitted properly to the experimental data without taking these two reactions into consideration.

This work is part of a systematic investigation of structure−reactivity correlations in palladium(II) chemistry.[1,2,10,42] Further kinetics studies on olefin complexes are in progress.[44]

Acknowledgment. We thank Dr. Ola F. Wendt for help with the NMR measurements. Valuable comments on structures of the olefin complexes from Dr. Carlaxel Andersson and financial support from the Swedish Natural Science Research Council are gratefully acknowledged.

Supporting Information Available: Observed and calculated pseudo-first-order rate constants of the slow and fast phases for the reaction between Pd(H$_2$O)$_4^{2+}$ and maleic acid at 25 °C and 2.00 M ionic strength (Table S1), absorbance for equilibrated solutions as a function of total maleic acid concentration (Figure S1), NMR spectrum of a 20 mM solution of the final product **C** and 2D NMR spectrum of **C** (Figure S2), and time-resolved spectra for the reaction between Pd(H$_2$O)$_4^{2+}$ and maleic acid (Figure S3) (5 pages). Ordering information is given on any current masthead page.

IC980072F

(43) Elding, L. I.; Gröning, A.-B. *Inorg. Chim. Acta* **1980**, *38*, 59−66.
(44) Plutino, M. R.; Otto, S.; Roodt, A.; Elding, L. I. *Inorg. Chem.*, submitted.
(45) Cramer, R. *Inorg. Chem.* **1965**, *4*, 445−447.
(46) Olsson, A.; Kofod, P. *Inorg. Chem.* **1992**, *31*, 183−186.